



Nikolay B. Volkov, Alexander I. Lipchak

Transport and optical properties of iron in the expanded and compressed states at high energy densities

*Institute of Electrophysics, Russian Academy of Science, Ural Branch
Amundsen Street 106, Yekaterinburg, 620016, Russia*

E-mail: nbv@iep.uran.ru

This research was funded by Russian Science Foundation and Government of Sverdlovsk Region, project No. 22-29-20058.



Outline

- 1. Introduction;*
- 2. Model;*
- 3. Results and Discussion;*
- 4. Conclusion.*



Introduction

The main objective of the present work is the studying the transport and optical properties of metals at high energy densities in expanded and compressed states. In this communication, we performed calculations for iron since it is used as a model material for an anode of gas gap controlled by pulsed laser radiation. In the model presented, a local equilibrium neutral metal is a plasma-like medium consisting of ions and electrons. Wherein ions and neutral atoms do not differ. The obtained thermophysical properties of iron at high energy densities are considered in detail in [N.B. Volkov, A.I. Lipchak. // Condensed Matter. – 2022. – Vol. 7, № 4: 61. – doi: [10.3390/condmat7040061](https://doi.org/10.3390/condmat7040061)].

**Onsager kinetic coefficients** $M_{0i}(V_a, T), K_{0i}(V_a, T), i = 0, 1, 2:$

$$M_{0\beta} = \frac{2me^{2-\beta}}{3\pi^2\hbar^3} \frac{\partial}{\partial\mu_1} \int_0^\infty \varepsilon^{\beta+1} l_{j,eff}(\varepsilon) (\exp((\varepsilon - \mu_1)/T) + 1)^{-1} d\varepsilon = \frac{2}{3\pi^2 e^\beta \hbar} \left(\frac{me^4}{\hbar^2} \right)^{\beta+1} \bar{T}^{\beta+1} \frac{\partial}{\partial x} \int_0^\infty \xi^{\beta+1} \bar{l}_{j,eff}(\xi) f_0(\xi - x) d\xi =$$

$$= \frac{1}{e^\beta \hbar} E_H^{\beta+1} \bar{M}_{0\beta}, \beta = 0, 1, 2; E_H = \frac{me^4}{\hbar^2}, \xi = \frac{\varepsilon}{T} = \frac{\bar{\varepsilon}}{\bar{T}}, x = \frac{\mu_1}{T} = \frac{\bar{\mu}_1}{\bar{T}}, \bar{T} = \frac{T}{E_H}, \bar{\mu}_1 = \frac{\mu_1}{E_H}, \bar{l}_{j,eff} = \frac{l_{j,eff}}{a_B}, a_B = \frac{\hbar^2}{me^2};$$

$$K_{0\beta} = \frac{2me^{2-\beta}}{3\pi^2\hbar^3} \frac{\partial}{\partial\mu_1} \int_0^\infty \varepsilon^{\beta+1} l_{q,eff}(\varepsilon) (\exp((\varepsilon - \mu_1)/T) + 1)^{-1} d\varepsilon = \frac{2}{3\pi^2 e^\beta \hbar} \left(\frac{me^4}{\hbar^2} \right)^{\beta+1} \bar{T}^{\beta+1} \frac{\partial}{\partial x} \int_0^\infty \xi^{\beta+1} \bar{l}_{q,eff}(\xi) f_0(\xi - x) d\xi =$$

$$= \frac{1}{e^\beta \hbar} E_H^{\beta+1} \bar{K}_{0\beta}, \beta = 0, 1, 2; \bar{l}_{q,eff} = \frac{l_{q,eff}}{a_B}.$$

$$\bar{M}_{0\beta} = \frac{\sqrt{2} z_i \bar{n}_i \bar{T}^{\beta-1/2}}{3} \frac{\frac{\partial}{\partial x} \int_0^\infty \xi^{\beta+1} \bar{l}_{j,eff}(\xi) f_0(\xi - x) d\xi}{F_{1/2}(x)}, \quad \bar{K}_{0\beta} = \frac{\sqrt{2} z_i \bar{n}_i \bar{T}^{\beta-1/2}}{3} \frac{\frac{\partial}{\partial x} \int_0^\infty \xi^{\beta+1} \bar{l}_{q,eff}(\xi) f_0(\xi - x) d\xi}{F_{1/2}(x)}, \quad \bar{n}_i = \frac{a_B^3}{V_a} = 1/\bar{V}_a.$$

Thermoelectric coefficient and electronic thermal conductivity:

$$\bar{\alpha} = x - \frac{\bar{M}_{01}}{\bar{T} \bar{M}_{00}} = x - \frac{\frac{\partial}{\partial x} \int_0^\infty \xi^2 \bar{l}_{j,eff}(\xi) f_0(\xi - x) d\xi}{\frac{\partial}{\partial x} \int_0^\infty \xi \bar{l}_{j,eff}(\xi) f_0(\xi - x) d\xi}; \quad \bar{\kappa} = \frac{1}{\bar{T}} \left(\bar{K}_{02} - \frac{\bar{M}_{01} \bar{K}_{01}}{\bar{M}_{00}} \right) + x \left(\frac{\bar{K}_{00} \bar{M}_{01}}{\bar{M}_{00}} - \bar{K}_{01} \right).$$



According to the diffraction model, the mean free path of electrons is written as

$$l_j^{-1} = \frac{m^2 n_i}{4\pi \hbar^4 k^4} \int_0^{2k} S_i^2(q) \left| \langle \mathbf{k} + \mathbf{q} | w_i | \mathbf{k} \rangle \right|^2 \varepsilon(q)^{-2} q^3 dq, \quad S_i^2(0) = S_{ii}^{-1}, \quad S_{ii} = \frac{K_{ii}(\rho, T)}{n_i T}, \quad K_{ii} = \rho \frac{\partial P_i}{\partial \rho} \Big|_T ;$$

$$\varepsilon(q) = 1 + k_D^{-2} q^{-2}; \quad w_i(r) = -\frac{e^2 z_i}{r} + \frac{e^2 (Z - z_i)}{r} \exp\left(-\frac{r}{r_c}\right), \quad r_c = \frac{Z - z_i}{Z^{3/2}} \left(\frac{\langle r^2 \rangle_a}{6} \right)^{1/2} ;$$

$$\left| \langle \mathbf{k} + \mathbf{q} | w_i | \mathbf{k} \rangle \right|^2 = \begin{cases} 16\pi^2 e^4 \left(\frac{z_i^2}{q^4} + \frac{(Z - z_i)^2 r_c^4}{(1 + q^2 r_c^2)^4} \right) & \text{for } \delta < 1 \\ \frac{16\pi^2 e^4 z_i^2}{q^4} & \text{for } \delta \geq 1 \end{cases} .$$

In the compressed state, the cutoff factor is the Debye wave number $q_D = (6\pi^2 / V_a)^{1/3} = q_{D0} \delta^{1/3}$,
so we write the structure factor in the form

$$S_i^2(q) = S_{ii}^{-1} \frac{\frac{q}{q_D} \frac{\Theta}{T}}{\exp\left(\frac{q}{q_D} \frac{\Theta}{T}\right) - 1} = S_{ii}^{-1} \frac{\frac{q}{q_D} \frac{\hbar \omega_D}{T}}{\exp\left(\frac{q}{q_D} \frac{\hbar \omega_D}{T}\right) - 1} \quad \text{for } \delta \geq 1.$$



$$\bar{l}_j(\bar{\varepsilon}_e) = \frac{\bar{\varepsilon}_e^2 S_{ii}(\bar{n}_i, \bar{T})}{\pi \bar{n}_i \Lambda_j(\langle \bar{\varepsilon}_e \rangle)}, \Lambda_j(\langle \bar{\varepsilon}_e \rangle) = \begin{cases} z_i^2 \Lambda_{j,c}(\langle \bar{\varepsilon}_e \rangle) \text{ for } \bar{V}_a \leq \bar{V}_{a0} (\delta = \bar{V}_{a0} / \bar{V}_a \geq 1) \\ z_i^2 \Lambda_{j,\text{ex1}}(\langle \bar{\varepsilon}_e \rangle) + (Z - z_i)^2 \Lambda_{j,\text{ex2}}(\langle \bar{\varepsilon}_e \rangle) \text{ for } \bar{V}_a > \bar{V}_{a0} (\delta < 1) \end{cases};$$

$$\bar{l}_q(\bar{\varepsilon}_e) = \frac{\bar{\varepsilon}_e^2 S_{ii}(\bar{n}_i, \bar{T})}{\pi \bar{n}_i \Lambda_q(\langle \bar{\varepsilon}_e \rangle)}, \Lambda_q(\langle \bar{\varepsilon}_e \rangle) = \begin{cases} z_i^2 \Lambda_{j,c}(\langle \bar{\varepsilon}_e \rangle) \left(1 + 3\pi^{-2} (\bar{k}_F \bar{q}_D^{-1})^2 (\bar{\omega}_D \bar{T}^{-1})^2 \right) \text{ for } \bar{V}_a \leq \bar{V}_{a0} (\delta \geq 1) \\ z_i^2 \Lambda_{j,\text{ex1}}(\langle \bar{\varepsilon}_e \rangle) + (Z - z_i)^2 \Lambda_{j,\text{ex2}}(\langle \bar{\varepsilon}_e \rangle) \text{ for } \bar{V}_a > \bar{V}_{a0} (\delta < 1) \end{cases},$$

whereat

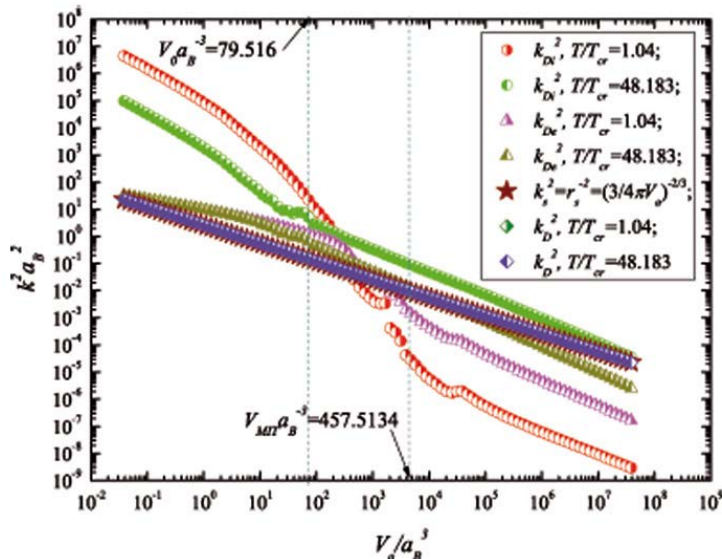
$$\Lambda_{j,c}(\langle \bar{\varepsilon}_e \rangle) = b_1^4 \int_0^{(8\langle \bar{\varepsilon}_e \rangle)^{1/2} / \bar{q}_D \bar{T}} \frac{\zeta^4 d\zeta}{(\exp(\zeta) - 1)(1 + b_1^2 \zeta^2)^2}, b_1 = \frac{\bar{q}_D}{\bar{k}_D} \frac{\bar{T}}{\bar{\omega}_D};$$

$$\Lambda_{j,\text{ex1}}(\langle \bar{\varepsilon}_e \rangle) = \int_0^{(8\langle \bar{\varepsilon}_e \rangle)^{1/2} / \bar{k}_D} \frac{\zeta^3 d\zeta}{(1 + \zeta^2)^2};$$

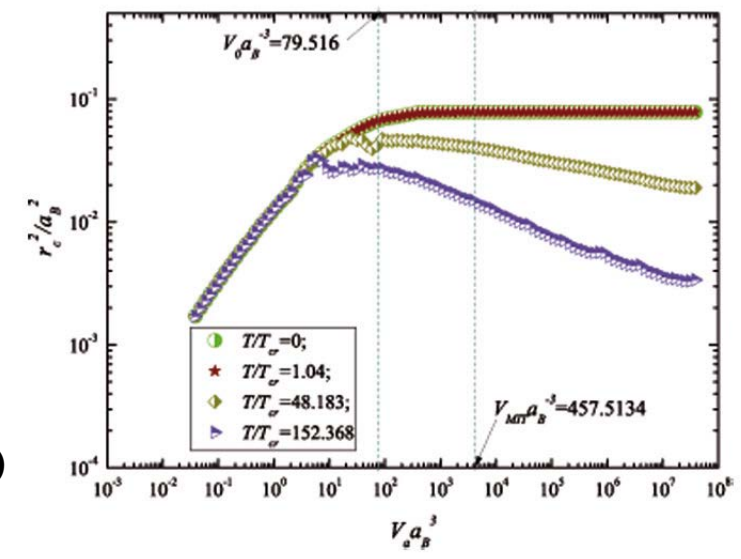
$$\Lambda_{j,\text{ex2}}(\langle \bar{\varepsilon}_e \rangle) = b_2^4 \int_0^{(8\langle \bar{\varepsilon}_e \rangle)^{1/2} / \bar{k}_D} \frac{\zeta^7 d\zeta}{(1 + b_2^2 \zeta^2)^2 (1 + \zeta^2)^2}, b_2 = \bar{r}_c \bar{k}_D.$$

$$\text{for } \bar{T} \ll \bar{\omega}_D \quad \bar{l}_j(\bar{\varepsilon}_e) = \frac{\bar{\varepsilon}_e^2 S_{ii}(\bar{n}_i, \bar{T})}{\pi \bar{n}_i \Lambda_j(\langle \bar{\varepsilon}_e \rangle)} = \frac{\bar{\varepsilon}_e^2 S_{ii}(\bar{n}_i, \bar{T})}{24\pi \bar{n}_i z_i^2 (\bar{q}_D \bar{T} / \bar{k}_D \bar{\omega}_D)^4} \propto \frac{\bar{\varepsilon}_e^2}{\bar{n}_i z_i^2 \bar{T}} \left(\frac{\bar{k}_D \bar{\omega}_D}{\bar{q}_D \bar{T}} \right)^4 \propto \bar{T}^{-5};$$

$$\bar{l}_q(\bar{\varepsilon}_e) = \frac{\bar{\varepsilon}_e^2 S_{ii}(\bar{n}_i, \bar{T})}{\pi \bar{n}_i \Lambda_j(\langle \bar{\varepsilon}_e \rangle) \left(1 + 3\pi^{-2} (\bar{k}_F \bar{q}_D^{-1})^2 (\bar{\omega}_D \bar{T}^{-1})^2 \right)} \equiv \frac{\pi \bar{\varepsilon}_e^2 S_{ii}(\bar{n}_i, \bar{T}) (\bar{k}_D \bar{\omega}_D)^4}{72 \bar{n}_i z_i^2 (\bar{q}_D \bar{T})^2 (\bar{k}_F \bar{\omega}_D)^2} \propto \bar{T}^{-3}.$$

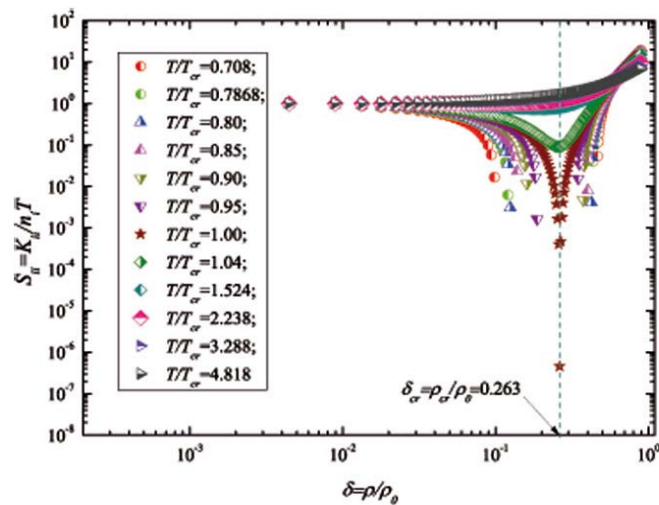


(a)

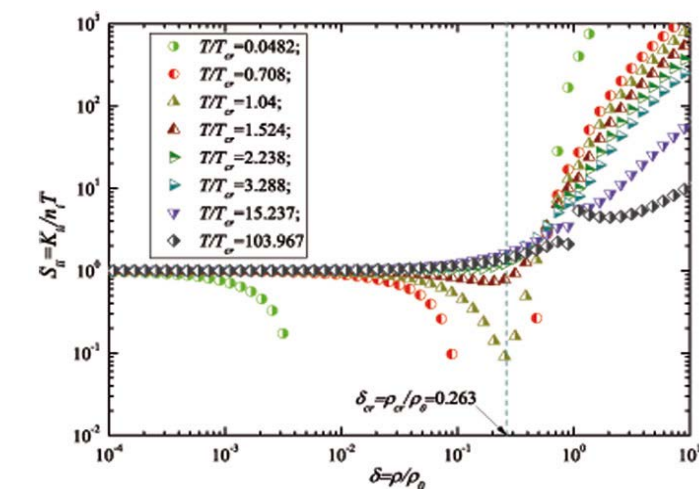


(b)

Figure 1. Squared Debye wave numbers (a) and square of screened radius of inner electrons (b).

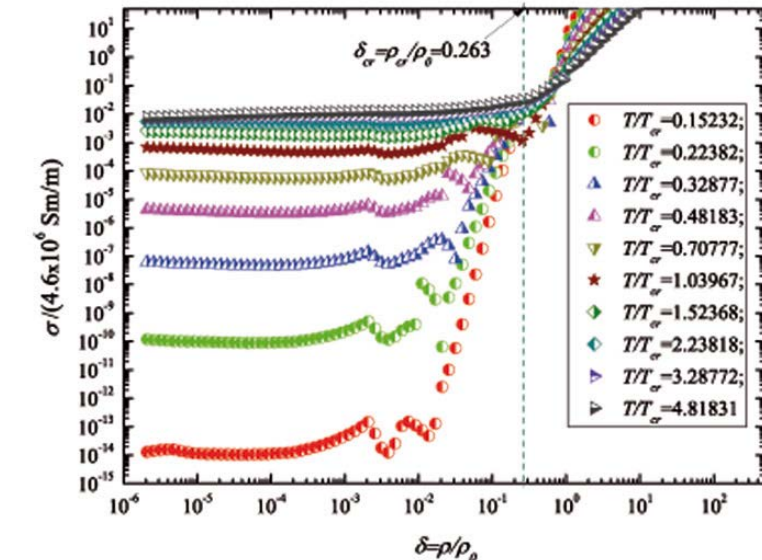


(a)

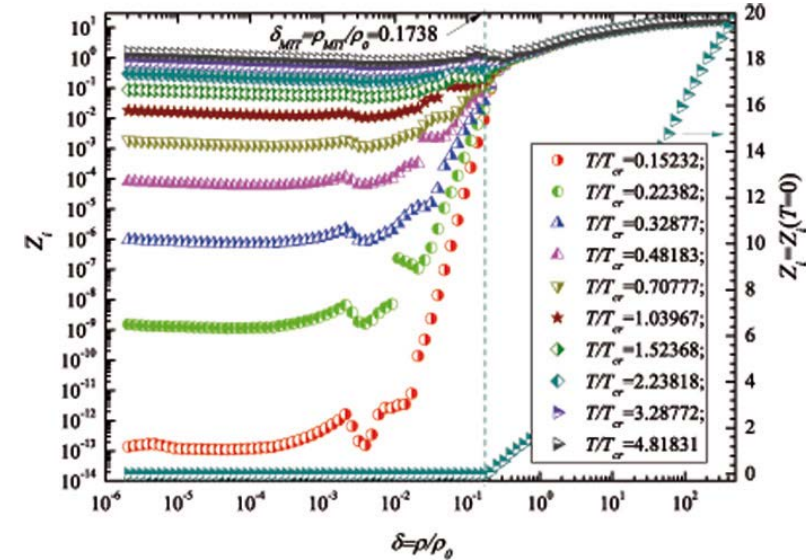


(b)

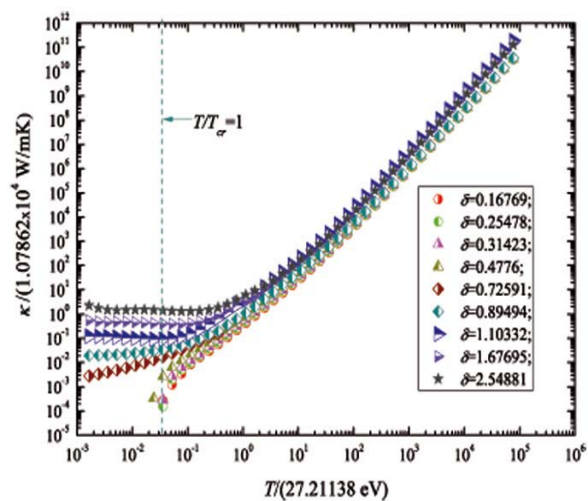
Figure 2. Iron long wave structure factor for small (a) and high temperatures (b).



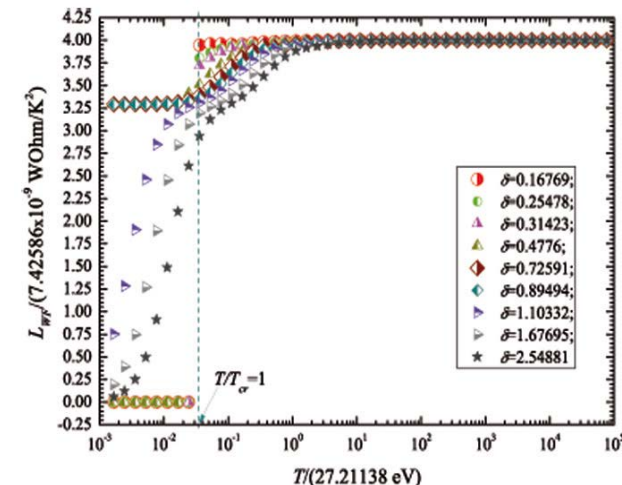
(a)



(b)

Figure 3. Iron electron conductivity (a) and number of electrons in an atomic cell (b).


(a)



(b)

Figure 4. Iron thermal conductivity (a) and Wiedemann-Franz ratio (b) from temperature.



Optical properties:

$$f = f_0 + \mathbf{v}_e \cdot \mathbf{f}_1 / v_e = f_0 + \mathbf{p} \cdot \mathbf{f}_1 / p, | \mathbf{v} \cdot \mathbf{f}_1 / v_e | \ll f_0 \Rightarrow$$

$$\Rightarrow \mathbf{f}_1(\omega) = -\frac{ev_e \frac{\partial f_0}{\partial \epsilon_e}}{-i\omega + \nu_{ei}(\epsilon_e)} \mathbf{E}(\omega) = \frac{e \left(\frac{2\epsilon_e}{m} \right)^{1/2} \frac{\partial f_0}{\partial \mu_1}}{-i\omega + (2\epsilon_e / m)^{1/2} l_{j,eff}^{-1}(\epsilon_e)} \mathbf{E}(\omega).$$

$$\begin{aligned} \mathbf{j}' &= 2e \int \mathbf{v}_e f \frac{d^3 \mathbf{p}}{(2\pi\hbar)^3} = \frac{(2m)^{3/2} e^2}{3m\pi^2\hbar^3} \frac{\partial}{\partial \mu_1} \int_0^\infty \frac{\epsilon_e^{3/2} f_0 d\epsilon_e}{-i\omega + \nu_{ei}(\epsilon_e)} \mathbf{E} = \frac{2z_i n_i e^2}{3m} \frac{\partial}{\partial \mu_1} \int_0^\infty \frac{\epsilon_e^{3/2} f_0 d\epsilon_e}{-i\omega + \nu_{ei}(\epsilon_e)} \mathbf{E} = \\ &= \left(\frac{2z_i n_i e^2}{3m} \frac{\partial}{\partial \mu_1} \int_0^\infty \frac{\nu_{ei}(\epsilon_e) \epsilon_e^{3/2} f_0 d\epsilon_e}{\omega^2 + \nu_{ei}^2(\epsilon_e)} + i\omega \frac{2z_i n_i e^2}{3m} \frac{\partial}{\partial \mu_1} \int_0^\infty \frac{\epsilon_e^{3/2} f_0 d\epsilon_e}{\omega^2 + \nu_{ei}^2(\epsilon_e)} \right) \mathbf{E} = \\ &= -i\omega \frac{\epsilon'(\omega) - 1}{4\pi} \mathbf{E} = -i\omega \frac{\epsilon_1(\omega) - 1 + i\epsilon_2(\omega)}{4\pi} \mathbf{E}. \end{aligned}$$



Where do we get:

$$\varepsilon_1(\omega) = 1 - \frac{2\omega_p^2}{3} \frac{\frac{\partial}{\partial \mu_1} \int_0^\infty \frac{\varepsilon_e^{3/2} f_0 d\varepsilon_e}{\omega^2 + \nu_{ei}^2(\varepsilon_e)}}{\int_0^\infty \varepsilon_e^{1/2} f_0 d\varepsilon_e} = 1 - \frac{2\bar{\omega}_p^2}{3} \frac{\frac{\partial}{\partial x} \int_0^\infty \frac{\xi^{3/2} f_0(\xi-x) d\xi}{\bar{\omega}^2 + \bar{\nu}_{ei}^2(\xi)}}{F_{1/2}(x)} \text{ - real part of the complex permittivity;}$$

$$\varepsilon_2(\omega) = \frac{2\omega_p^2}{3\omega} \frac{\frac{\partial}{\partial \mu_1} \int_0^\infty \frac{\nu_{ei}(\varepsilon_e) \varepsilon_e^{3/2} f_0 d\varepsilon_e}{\omega^2 + \nu_{ei}^2(\varepsilon_e)}}{\int_0^\infty \varepsilon_e^{1/2} f_0 d\varepsilon_e} = \frac{2\bar{\omega}_p^2}{3\bar{\omega}} \frac{\frac{\partial}{\partial x} \int_0^\infty \frac{\bar{\nu}_{ei}(\xi) \xi^{3/2} f_0(\xi-x) d\xi}{\bar{\omega}^2 + \bar{\nu}_{ei}^2(\xi)}}{F_{1/2}(x)} \text{ - imaginary part of the complex permittivity.}$$

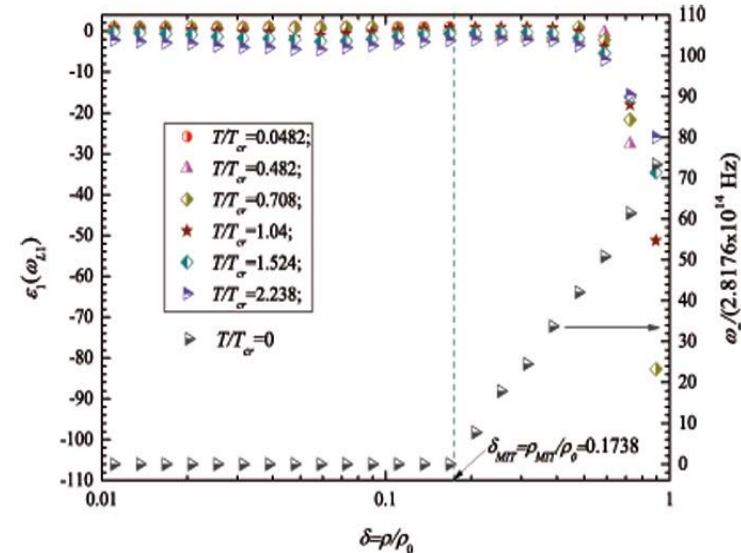
$$\varepsilon_1(\bar{\omega}_L) = 1 - \frac{2\bar{\omega}_p^2}{3\bar{\omega}_L^2} \frac{J_{11}(x) - J_{12}(x)}{F_{1/2}(x)}, \quad \varepsilon_2(\bar{\omega}_L) = \frac{2\bar{\omega}_p^2}{3\bar{\omega}_L^2} \frac{J_{21}(x) - J_{22}(x)}{F_{1/2}(x)};$$

$$J_{11}(x) = \int_0^\infty \frac{\bar{\omega}_L^2 \xi^{3/2} d\xi}{(\exp(\xi-x)+1)(\bar{\omega}_L^2 + \bar{\nu}_{ei}^2(\xi))}, \quad J_{12}(x) = \int_0^\infty \frac{\bar{\omega}_L^2 \xi^{3/2} d\xi}{(\exp(\xi-x)+1)^2 (\bar{\omega}_L^2 + \bar{\nu}_{ei}^2(\xi))};$$

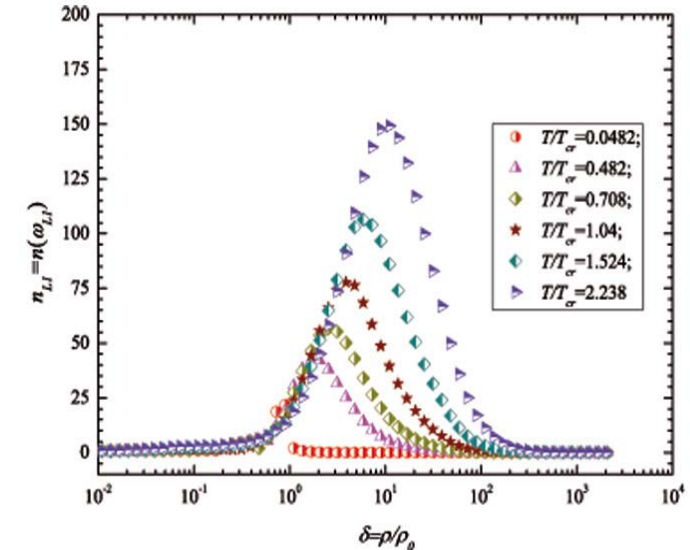
$$J_{21}(x) = \int_0^\infty \frac{\bar{\omega}_L \bar{\nu}_{ei}(\xi) \xi^{3/2} d\xi}{(\exp(\xi-x)+1)(\bar{\omega}_L^2 + \bar{\nu}_{ei}^2(\xi))}, \quad J_{22}(x) = \int_0^\infty \frac{\bar{\omega}_L \bar{\nu}_{ei}(\xi) \xi^{3/2} d\xi}{(\exp(\xi-x)+1)^2 (\bar{\omega}_L^2 + \bar{\nu}_{ei}^2(\xi))}.$$

The rate of change in the internal energy of a substance in the case of a dependence of its parameters on density and temperature due to heating by laser radiation can be written as:

$$Q_L(t, z) = I_L(t) \beta_L |E(t, z) / E_L(t)|^2 = I_L(t) \beta_L \exp\left(-\int_z^\infty \beta_L(z') dz'\right), \quad \beta_L = a_B^{-1} \bar{\beta}_L = a_B^{-1} \varepsilon_2(\bar{\omega}_L) \bar{\omega}_L / \bar{c}.$$

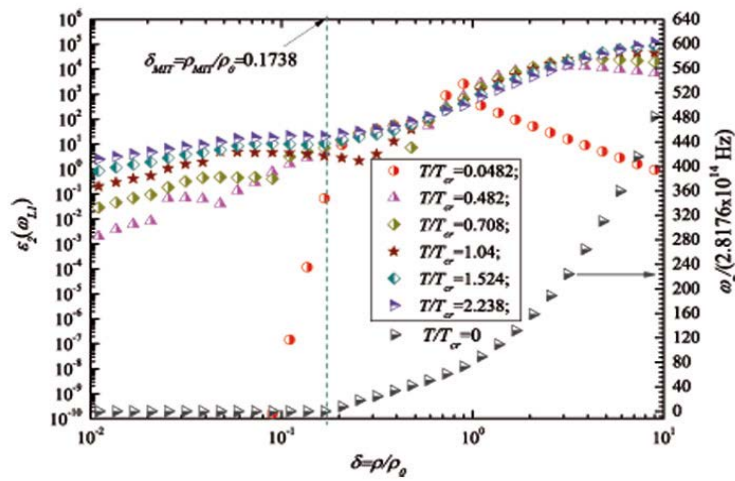


(a)

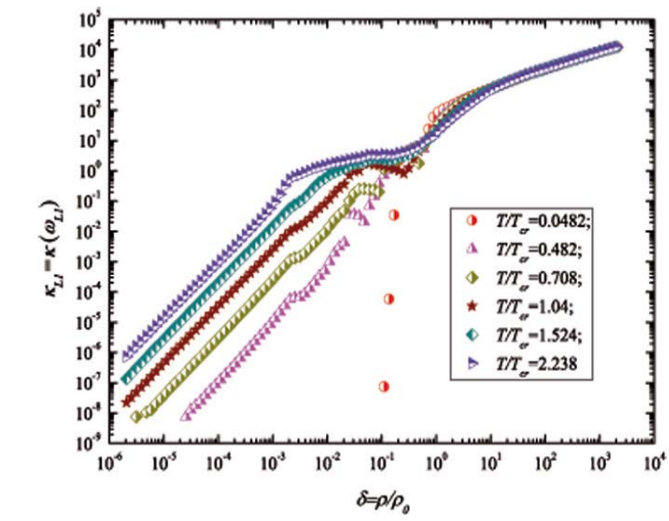


(b)

Figure 5. Iron real permittivity (a) and refraction index (b) for 1st harmonics of a laser radiation.

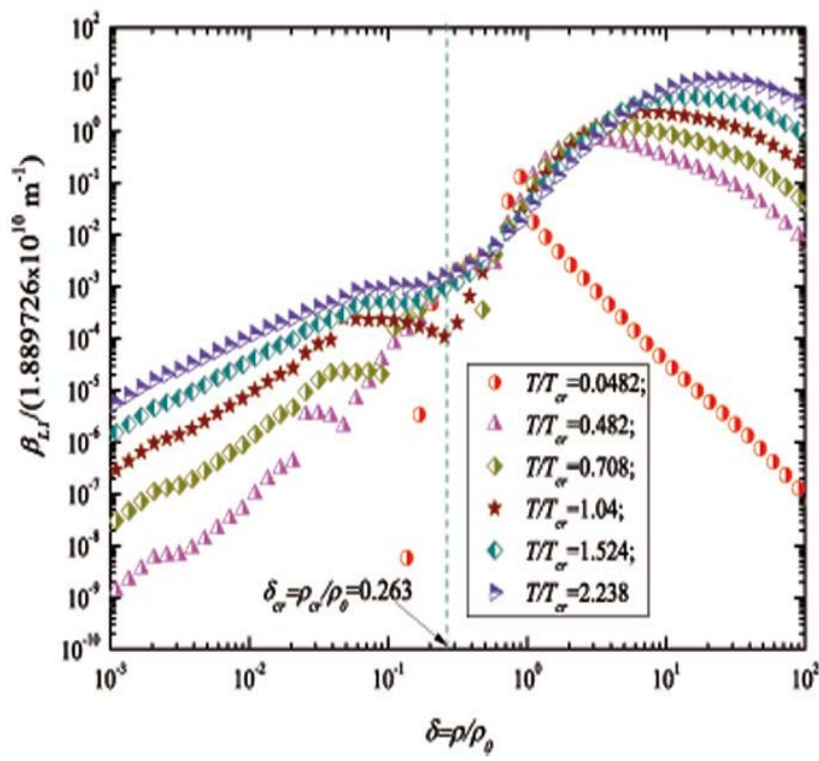


(a)

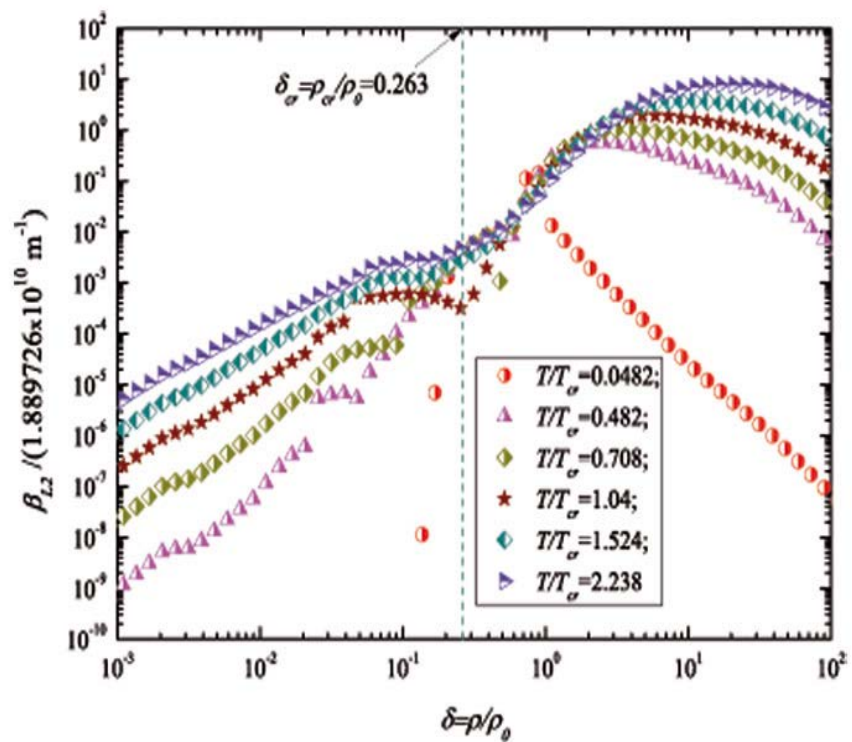


(b)

Figure 6. Iron imaginary permittivity (a) and absorption factor (b) for 1st harmonics.



(a)



(b)

Figure 7. Iron absorption coefficient for 1st (a) and 2nd (b) harmonics of a laser radiation.

Discussion

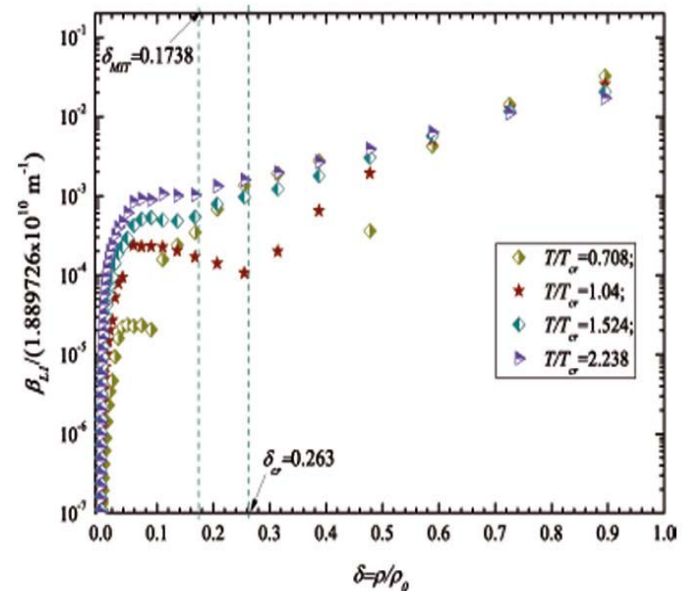
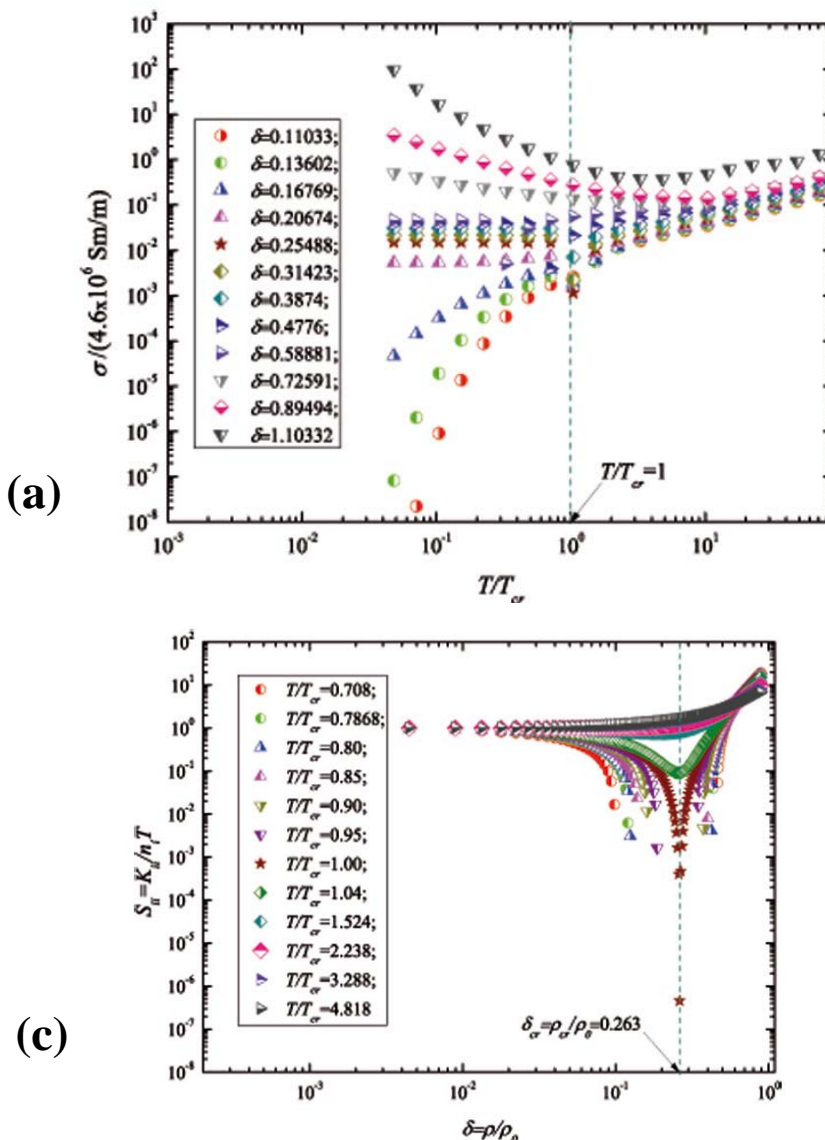


Figure 8. Iron conductivity (a), absorption coefficient (b) and long-wave structure factor (b).



(1) Curves fig. 8a, corresponding to low density values $\delta=0.11033-0.16769$, which are lower than the "metal-insulator" phase transition density at zero temperature, demonstrate a purely plasma behavior with increasing temperature.

(2) The curves corresponding to the density values $\delta=0.72591-1.10332$ demonstrate a continuous change in the nature of the electrical conductivity from metallic to plasma with increasing temperature.

(3) In recent experimental works [V.N. Korobenko, A.D. Rakhel. //*JETP*, **112**, 649 (2011); *Phys. Rev. B*, **85**, 014208 (2012)], it was reported that in the range of relative volume $V/V_0 = 3-5$ (relative density $\delta = 0.200-0.333$) in the pressure range $P = 20-25$ kbar, a change in the character of electrical conductivity was observed: from "metal" to "non-metal". The experimental pressure range corresponds to $P_{\text{exp}}/P_{\text{cr}}=2.424-3.03$ - [Korobenko&Rakhel]; $P_{\text{exp}}/P_{\text{cr}}=1.592-1.99$ - our work. **The experimental range $V/V_0 = 3-5$ correspond in Fig. 8a to three isodensities (isochores): (1) $\delta=0.20474$ ($V/V_0=4.837$); (2) $\delta=0.25488$ ($V/V_0=3.923$); (3) $\delta=0.31423$ ($V/V_0=3.182$).** The value (1) corresponds to the change in resistivity: $T/T_{\text{cr}}=0.708$ $\rho_e=29.03 \mu\Omega\text{m}$, $T/T_{\text{cr}}=1.04$ $\rho_e=141.77 \mu\Omega\text{m}$, $T/T_{\text{cr}}=1.524$ $\rho_e=24.96 \mu\Omega\text{m}$; (2) - $T/T_{\text{cr}}=0.708$ $\rho_e=14.513 \mu\Omega\text{m}$, $T/T_{\text{cr}}=1.04$ $\rho_e=186.887 \mu\Omega\text{m}$, $T/T_{\text{cr}}=1.524$ $\rho_e=20.57 \mu\Omega\text{m}$; (3) - $T/T_{\text{cr}}=0.708$ $\rho_e=10.329 \mu\Omega\text{m}$, $T/T_{\text{cr}}=1.04$ $\rho_e=99.38 \mu\Omega\text{m}$, $T/T_{\text{cr}}=1.524$ $\rho_e=16.209 \mu\Omega\text{m}$. The curves in Fig. 8b also indicate that at $\delta=0.25488$ ($V/V_0=3.923$) the absorption coefficient of laser radiation energy decreases sharply. Such a behavior of the specific resistance and energy absorption coefficient in the near-critical region of the "liquid-gas" phase transition is explained by the behavior of the structure factor, responsible for density fluctuations, in the near-critical and supercritical regions (see Fig. 8c).



Conclusions

The calculation method of transport and optical properties of metal in compressed and expanded states at high energy densities is proposed. The calculation results for iron are presented in tables for a wide range of temperatures and densities. The behavior of the electrical conductivity and absorption coefficient of laser radiation energy of iron in the region of the near- and over-critical point does not contradict the known experimental results shown.



*Many thanks for Your kind
attention!!!*